

Diabatic Mechanisms of Higher-Order Harmonic Generation in Solid-State Materials under High-Intensity Electric Fields

T. Tamaya,^{1,*} A. Ishikawa,² T. Ogawa,³ and K. Tanaka^{1,4,5}

¹*Department of Physics, Graduate School of Science, Kyoto University, Sakyo-ku, Kyoto 606-8502, Japan*

²*Department of Science for Advanced Materials, University of Yamanashi, 4-3-11 Takeda, Kofu, Yamanashi 400-8511, Japan*

³*Department of Physics, Osaka University, Toyonaka, Osaka 560-0043, Japan*

⁴*Institute for Integrated Cell-Material Sciences, Kyoto University, Sakyo-ku, Kyoto 606-8501, Japan*

⁵*CREST, Japan Science and Technology Agency, Kawaguchi, Saitama 332-0012, Japan*

(Received 13 December 2014; published 5 January 2016)

We theoretically investigate mechanisms of higher-order harmonic generation in solid-state materials under a high-intensity ac electric field. A new theoretical framework presented in this Letter holds the legitimacy of Bloch's theorem even under the influence of the high-intensity electric field and provides an exact treatment of the diabatic processes of Bloch electrons. Utilizing this framework, we first discovered that the diabatic processes, namely, ac Zener tunneling and semimetallization of semiconductors, are key factors for nonperturbative mechanisms of HHG. These mechanisms are classified by the field intensity and could be understood by an extended simple man model based on an analogy between tunnel ionization in gaseous media and Zener tunneling in semiconductors. These conclusions would stimulate the universal understanding of HHG mechanisms in both atomic and solid cases.

DOI: 10.1103/PhysRevLett.116.016601

Progress in the development of intense light sources has paved the way for strong-electric-field physics and stimulated investigations on nonperturbative nonlinear optical phenomena. The most prominent matter of these investigations is higher-order harmonic generation (HHG) in gaseous media and their potential utilities for optical technology, such as attosecond pulse generation and molecular orbit tomography, have been explored [1–3]. In recent years, HHG in solid-state materials has been experimentally observed focusing on characteristics different from those in atomic cases [4–8]. The differences are based on the periodic arrangement of atoms and collective properties of electrons in solid-state materials. Actually, these experiments show a band-gap dependence of a cutoff energy in HHG spectra [4,5], whose definition is a threshold between a constant intensity region (plateau region) and strong decay region, while, in atomic cases, that is determined by the relation with ionization energy of a single atom. Thus, HHG in solid-state materials is expected to have a different mechanism from that in atomic cases, and a clear understanding of such a mechanism will provide the possibility for opening new research fields of high-intensity optical technology.

For a clear understanding of mechanisms of HHG in solid-state materials, we should develop an exact treatment on the dynamics of the collective electrons under a high-intensity electric field. In solid-state materials where

a crystalline structure ensures the periodicity of the atomic potential, Bloch's theorem enables us to reduce the collective behavior of electrons to a single quasiparticle, which is called the Bloch electron [9]. Based on this scheme, we expect an exact investigation of the dynamics of Bloch electrons under the high-intensity ac electric field will unravel mechanisms of HHG. The high-intensity ac electric field causes a concurrence of excitation and transport processes of Bloch electrons, and therefore, the simultaneous treatment of these processes is necessary whose considerations enable discussions on diabatic processes of Bloch electrons such as Zener tunneling [10]. However, in spite of the simplicity of this problem, previous studies [5,11–17] have not provided reasonable treatments yet because of their invalid assumptions in constructing frameworks which would be summarized as follows.

In constructing the frameworks, we should take care of the legitimacy of Bloch's theorem under an influence of the high-intensity electric field. If the electric field is introduced in the form of a nonperiodic scalar potential $\phi = -e\mathbf{E}(t) \cdot \mathbf{x}$, the periodicity of atomic potential would be damaged and justification of Bloch's theorem is no longer expected to be adequate. Here, e is the electron charge, $\mathbf{E}(t)$ the external electric field, and \mathbf{x} the position of the electrons. In this case, Bloch functions cannot be regarded as a complete basis set and concepts of band structures and Bloch electrons become invalid [18,19]. These invalidities would greatly affect theoretical treatments of diabatic processes, as referred to in the previous works [18,19], and their influence on the perspective of HHG becomes emphasized especially when employing the

Published by the American Physical Society under the terms of the Creative Commons Attribution 3.0 License. Further distribution of this work must maintain attribution to the author(s) and the published article's title, journal citation, and DOI.

high-intensity ac electric field. In spite of these failures, some previous works [5,11,12], where transport processes are introduced by the scalar potential, constructed their theoretical frameworks based on assumptions of the completeness of Bloch functions as well as the concepts of band structures and Bloch electrons. For a correct perspective of HHG in the Bloch electron picture, it is essential to hold the periodicity of atomic potential even under an influence of the high-intensity electric field.

In the simultaneous treatments of excitation and transport processes of Bloch electrons, we also should take care of the justification of the classical kinetic equation $\hbar\dot{\mathbf{k}}(t) = -e\mathbf{E}(t)$, where \hbar and \mathbf{k} is the reduced Planck constant and Bloch wave vector. This equation is usually assumed in the treatments of transport processes of Bloch electrons and can be employed in theoretical frameworks by simple replacement of the Bloch wave vector \mathbf{k} with $\mathbf{k} - (e/\hbar c)\mathbf{A}(t)$, where the electric field is described as $\mathbf{E}(t) = -(1/c)\partial\mathbf{A}(t)/\partial t$. Here, c and $\mathbf{A}(t)$ are the velocity of light and a vector potential. For the simultaneous treatments of excitation and transport processes, the previous works [13–16] utilized this replacement in order to introduce transport processes of Bloch electrons, while excitation processes are involved in the usual dipole transition. However, as indicated by several researchers [20,21], this replacement is true only for single-band processes and should be violated by excitation processes such as Rabi flopping [22]. In the present situation, Bloch electron states are always described as a superposition of ground and excited states, and consequently, we should conclude that the previous works could not provide an accurate perspective of HHG due to an inaccurate expression of nonperturbative interaction of Bloch electrons. Moreover, the physical interpretation of the HHG mechanism based on Bloch oscillations [4,5,17], whose concept is true only for single-band processes, is no longer expected to be adequate. For the correct perspective, the theoretical frameworks should be constructed without assuming the conventional replacement of the Bloch wave vector.

In this Letter, avoiding invalid assumptions employed in the previous works [5,11–17], we clarify the nonperturbative mechanisms of HHG in solid-state materials. To treat the competition between excitation and transport processes of Bloch electrons accurately, our theoretical framework started from the Hamiltonian $H = (1/2m_0)[\mathbf{p} - e/c\mathbf{A}(t)]^2 + \sum_i V(x - R_i)$, where Bloch's theorem has not been applied yet. Here, m_0 is the electron mass, \mathbf{p} the momentum of bare electrons, and $V(x - R_i)$ the periodic core potential of atoms located at R_i . In this model, we employed a homogeneous electric field in the form of a vector potential rather than a scalar one, as has been proposed by Krieger and Iafrate in the case of the dc electric field [19]. An advantage of this treatment is that the Hamiltonian maintains its periodicity even including an influence of the high-intensity electric field. This ensures the validity of Bloch's theorem under the high-intensity

electric field, and consequently, Bloch functions are expected to be a complete basis set and concepts of band structures and Bloch electrons become adequate. The legitimacy of Bloch's theorem, including the high-intensity electric field, enables us to expect that there will be temporally changed band structures linked to an ac electric field, whereas the Bloch wave vector \mathbf{k} will not change and be a kinetic constant [21]. We should take care of the Hamiltonian not always leading to the classical kinetic equation for the Bloch wave vector $\hbar\dot{\mathbf{k}}(t) = -e\mathbf{E}(t)$, especially when treating excitation and transport processes together. Based on this scheme, we first discovered that diabatic processes, namely, ac Zener tunneling and semimetallization of semiconductors, determine the characteristics of HHG in solid-state materials. These considerations would provide new understanding of the fundamental mechanisms of HHG in semiconductors.

In constructing our theoretical framework, we suppose two-dimensional semiconductors which are referred to in the recent experiment [5], while conclusions presented in this Letter have no dependence on the dimensionality. Starting from this assumption and focusing only on conduction and valence bands, we could introduce a Hamiltonian described by $H = H_0 + H_I$ [23], where

$$H_0 = \sum_{\mathbf{k}} [(E_{\mathbf{k}}^e + E_g/2)e_{\mathbf{k}}^\dagger e_{\mathbf{k}} + (E_{\mathbf{k}}^h + E_g/2)h_{-\mathbf{k}}^\dagger h_{-\mathbf{k}}], \quad (1)$$

$$H_I = \hbar\Omega_R(t)\sum_{\mathbf{k}} \cos\theta_{\mathbf{k}}(e_{\mathbf{k}}^\dagger e_{\mathbf{k}} + h_{-\mathbf{k}}^\dagger h_{-\mathbf{k}} - 1) + i\hbar\Omega_R(t)\sum_{\mathbf{k}} \sin\theta_{\mathbf{k}}(e_{\mathbf{k}}^\dagger h_{-\mathbf{k}}^\dagger - h_{-\mathbf{k}} e_{\mathbf{k}}). \quad (2)$$

Here, $E_{\mathbf{k}}^\sigma = \hbar^2\mathbf{k}^2/2m_\sigma$ ($\sigma = e, h$) are the kinetic energies of electrons and holes, E_g is the band-gap energy, $e_{\mathbf{k}}(h_{\mathbf{k}})$ and $e_{\mathbf{k}}^\dagger(h_{\mathbf{k}}^\dagger)$ are the annihilation and creation operators of electrons (holes), $\theta_{\mathbf{k}}$ is the argument of the Bloch wave vector \mathbf{k} , and $\Omega_R(t) = \Omega_{R0} \exp[-(t - t_0)^2/\tau^2] \cos(\omega_0 t)$ is the Rabi frequency [28] where the intensity of the electric field is renormalized in Ω_{R0} . Throughout this Letter, we will fix the parameters of the incident electric field as $t_0 = 12\pi/\omega_0$ and $\tau = 4\pi/\omega_0$. The first term on the right hand side in Eq. (2) indicates the intraband transition in which the Bloch wave vector \mathbf{k} is a kinetic constant and it can be renormalized in the single-particle energy $\epsilon_{\mathbf{k}}^\sigma$, where $\epsilon_{\mathbf{k}}^\sigma(t) = E_{\mathbf{k}}^\sigma + E_g/2 + \hbar\Omega_R(t) \cos\theta_{\mathbf{k}}$. These modifications caused by an ac electric field mean a temporal variation of the band structure, which is consistent with the above discussion. The variations can be derived from temporal changes of diagonal matrix elements originating from the light-matter interaction that is usually ignored in nonlinear optics [22,28]. Moreover, comparing with the Landau-Zener model [29], we can interpret the Hamiltonian to include diabatic processes such as above-threshold ionization and Zener tunneling [10]. The second term of the right side in Eq. (2) indicates a dipole transition causing multiphoton absorption and Rabi flopping, which are nonlinear optical phenomena [22,28]. The factors $\sin\theta_{\mathbf{k}}$ and $\cos\theta_{\mathbf{k}}$

are derived from the form factor reflecting microscopic information on the arrangement of atoms in crystals.

Considering the above-mentioned Hamiltonian, we can derive time evolution equations for populations $f_k^\sigma = \langle \sigma_k^\dagger \sigma_k \rangle$ and polarization $P_k = \langle h_{-k}^\dagger e_k \rangle$ with the Bloch wave vector k as

$$i \frac{\partial}{\partial t} P_k = [\epsilon_k^e(t) + \epsilon_k^h(t)] P_k + i \Omega_R(t) \sin \theta_k [1 - f_k^e - f_k^h] - i \gamma_t P_k, \quad (3)$$

$$\frac{\partial}{\partial t} f_k^\sigma = 2 \text{Im} i \Omega_R(t) \sin \theta_k P_k^\dagger - \gamma_l f_k^\sigma. \quad (4)$$

Here, γ_t and γ_l are the transverse and longitudinal relaxation constants, and throughout this study, they will be fixed to $\gamma_t = 0.1\omega_0$ and $\gamma_l = 0.01\omega_0$, respectively. These values are estimated by the recent experimental situation [5] where the incident frequency is several tens of terahertz, while the dephasing and the energy relaxation time are regarded as a few tens of femtoseconds and a few picoseconds, respectively. The numerical solutions of these equations give the time evolutions of distributions of the carrier densities and polarization in two-dimensional k space. The distributions arise from a dipole transition under the anisotropic modification of the band structure characterized by the factor $\hbar \Omega_R(t) \cos \theta_k$, and consequently, they show anisotropic behavior in k space linked to the direction of the electric field [23]. Therefore, we expect that the intraband processes lead to carrier transport (wave packet dynamics), and the time evolution of the current can be calculated using the definition $J(t) = -c \langle \partial H_I / \partial A \rangle = \sum_k [(1 - f_k^e - f_k^h) \cos \theta_k - 2 \text{Im}(P_k) \sin \theta_k]$. Accordingly, we can derive higher-order harmonic spectra from the definition $I(\omega) = |\omega J(\omega)|^2$, where $J(\omega)$ is the Fourier transform of $J(t)$, and discuss the dependence of higher-order harmonic spectra on the intensity of the incident electric field corresponding to the Rabi frequency Ω_{R0} .

The numerical results show that the characteristics of HHG are changed, depending on the Rabi frequency. In this study, we always assume a situation where $\omega_0 \ll E_g/\hbar$. At the beginning, in the multiphoton absorption regime where a perturbative treatment of light-matter interaction is assured [Fig. 1(a)], we could identify the well-known characteristics in HHG spectra [Fig. 2(a)], i.e., the conventional relation of nonlinear optics $I_N \propto |P_N|^2 \propto |E_0|^{2N}$ [22] and strong generation of only odd-order harmonics which is explained by HHG emitted in each half-cycle period of the incident electric field [1]. With increasing the Rabi frequency, unconventional nonperturbative mechanisms of HHG should be emphasized, as shown in Figs. 1(b) and 1(c), where excitation processes are dominated by Zener tunneling and semimetallization processes, respectively. To understand these regimes easily, in these figures, we assume uniform modifications of band structures described by $\epsilon_k^\sigma(t) = E_k^\sigma + E_g/2 + \hbar \Omega_R(t)$, while the anisotropic factor $\cos \theta_k$ only causes dynamics of the wave packet in k space. The threshold of the field intensity between the multiphoton

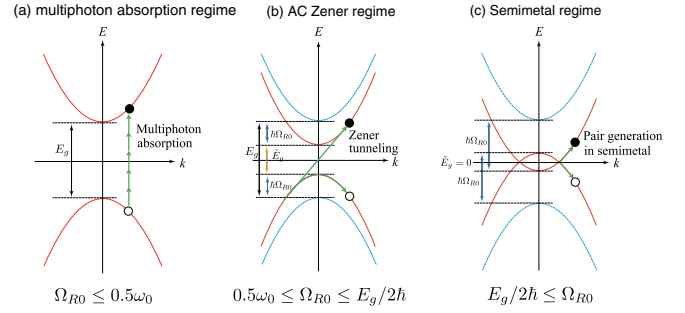


FIG. 1. Schematic diagrams of HHG mechanisms depending on the electric field intensity. (a) Multiphoton absorption regime, (b) ac Zener regime, and (c) semimetal regime. Red and blue lines show band dispersion with and without modification due to an external electric field. Green lines show excitation processes of Bloch electrons.

absorption regime and the ac Zener regime can be found as the boundary when a perturbative theory becomes inadequate, which is derived as $\Omega_{R0} = 0.5\omega_0$ [30], while that between the ac Zener regime and the semimetal regime can be estimated as the boundary when the sum of the renormalized single-particle energy is zero: $\epsilon_{k=0}^e + \epsilon_{k=0}^h = 0$, i.e., $E_g/2\hbar = \Omega_{R0}$. In the following, we will discuss the characteristics and mechanisms of HHG in each regime.

Figure 2(b) shows the higher-order harmonic spectra in the ac Zener regime, where the band-gap energies are $E_g = 10\hbar\omega_0$ (blue line) and $E_g = 5\hbar\omega_0$ (red line) in the case of $\Omega_{R0} = 2\omega_0$. We find that the spectra are divided into plateau and decay regions, and the plateau region becomes broader with increasing band-gap energy. This mechanism can be understood by an analogy between Zener tunneling and tunnel ionization processes in gaseous media [1]. The threshold between the plateau and decay regions is called cutoff energy, which corresponds to the maximum energy of the electron-hole pair accelerated by the electric field after the pair excitation. We will consider a simple man model [1,31] in semiconductors, as shown in Fig. 3(a), and estimate the cutoff energy E_C as $E_C = 2 \times (\tilde{E}_g/2 + \hbar\Omega_{R0} + 3.2U_p) = E_g + 2 \times 3.2U_p$, where $\tilde{E}_g = E_g - 2\hbar\Omega_{R0}$ is the renormalized band-gap energy modulated by the effect of intraband transition and U_p is a ponderomotive energy which represents the quiver energy of a free particle averaged over one cycle. Here, the factor 2 is derived from the two kinds of particles (electrons and holes). In addition, considering the correspondence of the ac Stark shift and the ponderomotive shift, we can introduce the relation $|U_p| = (1/4)\hbar\Omega_{R0}$ [30], and then the cutoff energy can be derived as $E_C \approx E_g + 1.6\hbar\Omega_{R0}$. This equation reveals that the cutoff energy shifts toward the higher-energy side, in short, the plateau region becomes broader, as the band-gap energy becomes larger. Assuming an experimental situation where an ac electric field of 30 THz is applied to GaSe and the perturbative treatments are becoming inadequate, we can expect the Rabi frequency and band-gap energy to be

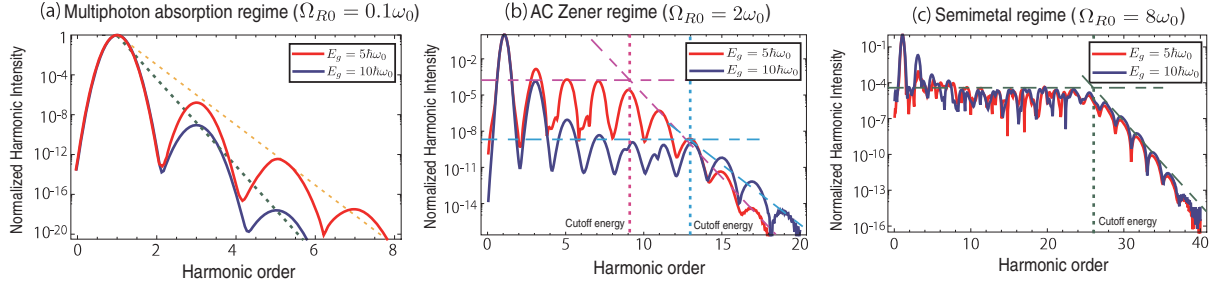


FIG. 2. Higher harmonic spectra generated from two-dimensional semiconductors: (a) Multiphoton absorption regime, (b) ac Zener regime, and (c) semimetal regime. Red and blue lines show spectra in the case of $E_g = 5\hbar\omega_0$ and $E_g = 10\hbar\omega_0$, respectively.

$\Omega_{R0} \approx 0.5\omega_0$ and $E_g \approx 16\hbar\omega_0$. Accordingly, we can conclude that the cutoff energy is roughly determined by the band-gap energy, which is consistent with recent experimental results [5].

Figure 2(c) shows the higher-order harmonic spectra in the semimetal regime, where the band-gap energies are $E_g = 10\hbar\omega_0$ (blue line) and $E_g = 5\hbar\omega_0$ (red line) in the case of $\Omega_{R0} = 8\omega_0$. Different from multiphoton absorption and ac Zener regimes, the higher-order harmonics show a characteristic of white spectrum which masks the odd-order harmonics, and, moreover, the cutoff energy no longer depends on the band-gap energy. The generation of the white higher-order harmonics means the emission law in each half cycle is broken. This half-cycle emission law can also be interpreted as temporal interference of HHG waves emitted dependently in a half cycle of the incident electric field [32,33]. On the basis of this idea, the breaking of the emission law is due to the overlap between the conduction and valence bands by the semimetallization for a long interval, which disturbs the interference that generates only odd-order harmonic spectra. To explain the independence of the cutoff energy from the band-gap energy, we extend the simple man model, as shown in Fig. 3(b). In this model,

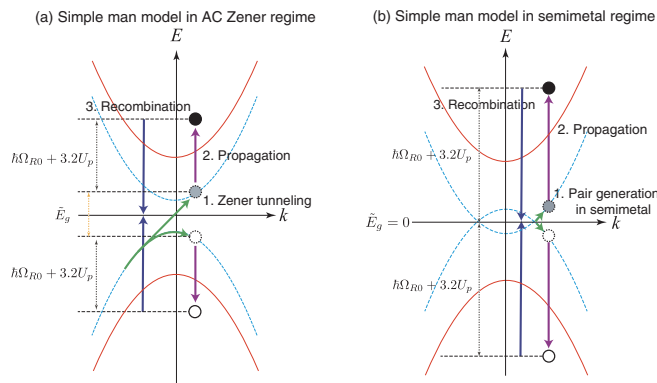


FIG. 3. Schematic diagram of simple man models in (a) ac Zener regime and (b) semimetal regime. In these figures, the simple man models are composed of three steps: (1) generation of carriers, (2) acceleration, and (3) recombination. The main difference between these diagrams is caused by generation processes. In the ac Zener regime, carriers are excited by Zener tunneling, while in the semimetallization regime, carriers are excited when the band gap becomes closed.

carriers are generated when the band gap becomes zero, after which they are accelerated and finally recombine. From such processes, we can derive the cutoff energy as $E_C = 2 \times (\hbar\Omega_{R0} + 3.2U_p) \approx 3.6\hbar\Omega_{R0}$, and this equation reveals that the cutoff energy no longer depends on the band-gap energy. These considerations are based on simple two-band models and their justification is assured by a condition that the band-gap energy is much smaller than energy differences between the first and the second conduction bands. Therefore, our results would be identified in experiments with several materials such as GaAs and InN.

Figures 4(a) and 4(b) show the dependence of the cutoff frequency ω_C on the Rabi frequency, as estimated from the numerical results (purple solid circles) and the simple man model (blue and red lines) in the cases of (a) $E_g = 5\hbar\omega_0$ and (b) $E_g = 10\hbar\omega_0$. In the numerical calculation, the cutoff frequency ω_C is determined as the threshold energy between the plateau and decay regions, where the plateau region is defined from a condition that the harmonic intensities become less than 10% compared with the previous and later orders. We found a crossover between ac Zener and semimetal regimes from the dependence of the cutoff energy on the Rabi frequency.

Finally, we will clarify the dephasing effect on the HHG spectra whose importance is discussed in the previous works [13,14]. The increasing dephasing effects enable us to presume the disappearance of temporal interference of HHG waves, each of which is emitted dependently in a half cycle. Therefore, when employing the dephasing value of $\gamma_t \approx \omega_0$, we expect the HHG spectra to be characterized by

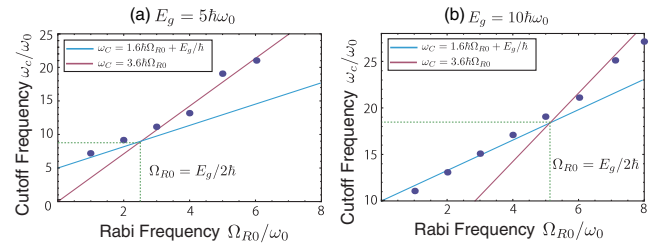


FIG. 4. The cutoff-frequency transition from ac Zener to semimetal regimes depending on the Rabi frequency in the case of $E_g = 10\hbar\omega_0$ and $E_g = 5\hbar\omega_0$. Blue and red lines show cutoff laws in ac Zener and semimetallization regimes. Purple dots indicate the cutoff frequency estimated from numerical results.

the single-cycle excitation processes, and consequently, the spectra widths become broader [34]. We identified this conjecture by performing our numerical calculations. This characteristic becomes important when considering HHG in the semimetal regime. In this regime, the increasing dephasing effect changes noisy continuumlike spectra into clean odd-ordered ones. We emphasize that the cutoff laws derived in this Letter are not influenced by the dephasing effect as long as a range of $0 \leq \gamma_t \leq \omega_0$ is being considered, which covers recent experimental situations [4–8].

In this Letter, based on an exact treatment of diabatic processes of Bloch electrons, we first discovered non-perturbative mechanisms of HHG in solid-state materials. In our theoretical framework, employing an external electric field in the form of a vector potential rather than the scalar one, the justification of Bloch's theorem is ensured even under the influence of the high-intensity electric field. In this scheme, temporally changed band structures linked to an ac electric field characterize diabatic processes of Bloch electrons. Utilizing this framework, we revealed these diabatic processes, namely, ac Zener tunneling and the semimetallization of semiconductors, determine properties of HHG spectra whose cutoff laws are in the form of $E_C = E_g + 1.6\hbar\Omega_{R0}$ and $E_C = 3.6\hbar\Omega_{R0}$, respectively. The cutoff laws could be understood based on analogies between Zener tunneling and tunnel ionization processes, as well as semimetallization of semiconductors and over-the-barrier ionization processes [30,35], where band-gap energy and Bloch electrons correspond to the ionization energy and bare electrons, respectively. The analogies presented in this Letter would provide possibilities for the universal understanding of HHG mechanisms in both atomic and solid cases, and consequently, propose the availability of the same method for coherent control such as a polarization gating [2,36].

The authors thank Y. Onishi for fruitful discussions. This work was supported by a Grant-in-Aid for Scientific Research on Innovative Areas, titled ‘‘Optical science of dynamically correlated electrons (DYCE)’’ (Grant No. 20104007), a Grant-in-Aid for Scientific Research (A) (Grant Nos. 26247052 and 23244065), a Grant-in-Aid for Scientific Research (B) (Grant No. 26287087), and an ImPACT Program of the Council for Science, Technology and Innovation (Cabinet Office, Government of Japan).

*ttamaya@scphys.kyoto-u.ac.jp

- [1] T. Brabec and F. Krausz, *Rev. Mod. Phys.* **72**, 545 (2000).
- [2] P. B. Corkum, N. H. Burnett, and M. Y. Ivanov, *Opt. Lett.* **19**, 1870 (1994).
- [3] J. Itatani, J. Levesque, D. Zeidler, H. Niikura, H. Pépin, J. C. Kieffer, P. B. Corkum, and D. M. Villeneuve, *Nature (London)* **432**, 867 (2004).
- [4] S. Ghimire, A. D. DiChiara, E. Sistrunk, P. Agostini, L. F. DiMauro, and D. A. Reis, *Nat. Phys.* **7**, 138 (2011).
- [5] O. Schubert *et al.*, *Nat. Photonics* **8**, 119 (2014).
- [6] T. T. Luu, M. Garg, S. Yu. Kruchinin, A. Moulet, M. Th. Hassan, and E. Goulielmakis, *Nature (London)* **521**, 498 (2015).
- [7] G. Vampa, T. J. Hammond, N. Thiré, B. E. Schmidt, F. Légaré, C. R. McDonald, T. Brabec, and P. B. Corkum, *Nature (London)* **522**, 462 (2015).
- [8] M. Hohenleutner, F. Langer, O. Schubert, M. Knorr, U. Huttner, S. W. Koch, M. Kira, and R. Huber, *Nature (London)* **523**, 572 (2015).
- [9] C. Kittel, *Introduction to Solid State Physics* (Wiley, New York, 1996).
- [10] C. Zener, *Proc. R. Soc. A* **145**, 523 (1934).
- [11] D. Golde, T. Meier, and S. W. Koch, *Phys. Rev. B* **77**, 075330 (2008).
- [12] D. Golde, M. Kira, T. Meier, and S. W. Koch, *Phys. Status Solidi (b)* **248**, 863 (2011).
- [13] G. Vampa, C. R. McDonald, G. Orlando, D. D. Klug, P. B. Corkum, and T. Brabec, *Phys. Rev. Lett.* **113**, 073901 (2014).
- [14] G. Vampa, C. R. McDonald, G. Orlando, P. B. Corkum, and T. Brabec, *Phys. Rev. B* **91**, 064302 (2015).
- [15] P. G. Hawkins, M. Yu. Ivanov, and V. S. Yakovlev, *Phys. Rev. A* **91**, 013405 (2015).
- [16] C. R. McDonald, G. Vampa, P. B. Corkum, and T. Brabec, *Phys. Rev. A* **92**, 033845 (2015).
- [17] S. Ghimire, A. D. DiChiara, E. Sistrunk, G. Ndabashimiye, U. B. Szafruga, A. Mohammad, P. Agostini, L. F. DiMauro, and D. A. Reis, *Phys. Rev. A* **85**, 043836 (2012).
- [18] G. Nenciu, *Rev. Mod. Phys.* **63**, 91 (1991).
- [19] J. B. Krieger and G. J. Iafrate, *Phys. Rev. B* **33**, 5494 (1986).
- [20] G. Wannier, *Rev. Mod. Phys.* **34**, 645 (1962).
- [21] C. Kittel, *Quantum Theory of Solids* (Wiley, New York, 1963), p. 190.
- [22] Y. R. Shen, *The Principles of Nonlinear Optics* (Wiley, New York, 1984).
- [23] See Supplemental Material at <http://link.aps.org/supplemental/10.1103/PhysRevLett.116.016601>, which includes Refs. [10,24–30], for derivation of the Hamiltonian.
- [24] P. Y. Yu and M. Cardona, *Fundamentals of Semiconductors: Physics and Material Properties*, 3rd ed. (Springer, New York, 2001).
- [25] E. Malic, T. Winzer, E. Bobkin, and A. Knorr, *Phys. Rev. B* **84**, 205406 (2011).
- [26] T. Stroucken, J. H. Grönqvist, and S. W. Koch, *Phys. Rev. B* **84**, 205445 (2011).
- [27] M. Lombardi, P. Labastie, M. C. Bordas, and M. Broyer, *J. Chem. Phys.* **89**, 3479 (1988).
- [28] H. Haug and S. W. Koch, *Quantum Theory of the Optical and Electronic Properties of Semiconductors* (World Scientific, Singapore, 1990).
- [29] C. Cohen-Tannoudji, B. Diu, and F. Laloe, *Quantum Mechanics* (Wiley, New York, 1977), Vol. 1.
- [30] J. H. Eberly, J. Javanainen, and K. Rzażewski, *Phys. Rep.* **204**, 331 (1991).
- [31] P. B. Corkum, *Phys. Rev. Lett.* **71**, 1994 (1993).
- [32] K. L. Ishikawa, *Phys. Rev. A* **74**, 023806 (2006).
- [33] D. G. Arbó, K. L. Ishikawa, K. Schiessl, E. Persson, and J. Burgdörfer, *Phys. Rev. A* **81**, 021403(R) (2010).
- [34] D. Golde, T. Meier, and S. W. Koch, *J. Opt. Soc. Am. B* **23**, 2559 (2006).
- [35] X. M. Tong and C. D. Lin, *J. Phys. B* **38**, 2593 (2005).
- [36] G. Sansone *et al.*, *Science* **314**, 443 (2006).